JOURNAL OF MATERIALS SCIENCE 30 (1995) 5872–5878

Effect of plastic coating on fibre–matrix interface debonding

GUI-YING LU
Department of Materials Science and Engineering, Ohio State University, Columbus, OH 43210, USA,

YIU-WING MAI*
Centre for Advanced Materials Technology, Department of Mechanical and Mechatronic Engineering, University of Sydney, NSW 2006, Australia

A theoretical model including the effect of plasticity of the coating material on the single-fibre pull-out test has been developed. Both hardening and perfectly plastic coatings were modelled and the calculations have provided much information on the debond and maximum pull-out stresses. For both SiC fibre–glass and carbon fibre–epoxy systems, a stiff coating reduces substantially the partial debonding stress, but a soft coating increases it markedly. Although a higher coating yield stress increases the partial debonding stress slightly, the maximum pull-out stress is independent of the coating.

1. Introduction

Fibre coatings dominate the mechanical behaviour of fibre-reinforced composites. Recently, the effects of interfacial conditions on toughness and energy dissipation have been addressed by a number of investigators [1–6]. It is noted that to obtain optimum mechanical, chemical and physical properties, fibres need to be coated. Fibre coatings may be used to control the bond strength between fibre and matrix, permitting interface debonding and fibre pull-out to occur, thus enhancing the total fracture toughness of the composite. Also, they are used to improve the fibre resistance to oxidation and/or prevent chemical reaction between fibre and matrix. These are the thermomechanical roles of fibre coatings.

Di'anselmo *et al.* [7] have used finite element analysis to compare the effects of the interphase with different moduli and thicknesses on local stresses and energy distribution for a model E-glass fibre–epoxy matrix composite. It is concluded that the moduli and thicknesses of the interphase have a strong effect on the stress and energy distribution and the softer interphase has a lower energy release rate. The analysis performed is linear, and does not include friction or residual clamping stress. To model interface debonding and matrix cracks, for simplicity, the elements corresponding to the crack region are deleted. In their recent work on an E-glass fibre embedded in a polyester matrix with a silane coating (soft interphase) and without coating, Connelly *et al.* [8] found that, without the soft interphase, failure occurs by crack propagation into the matrix. But with a soft interphase, interfacial debonding occurs initially, followed by crack propagation into the matrix at the fibre break.

Sottos *et al.* [9] have carried out an experimental study and performed theoretical evaluation of the influence of the interphase on local thermal displacements. A thermal displacement solution is derived for a three-phase, finite composite cylinder model using a displacement potential approach, with perfect bond condition. Their model does not consider the residual stress which develops as a result of the fabrication process.

Mital and Chamis [10] have conducted a simulation of the single-fibre push-out process using a three-dimensional finite element method. The interphase material is replaced by an anisotropic material with a greatly reduced shear modulus, the fibre pushout load at any temperature (corresponding to different interphases) are calculated. In their model, the thickness and properties of the interphases have not been included.

Observations have indicated that coatings can be classified into four groups [2]: (a) ductile coatings that do not debond; (b) ductile coatings that debond; (c) brittle coatings that debond at one interface; and (d) brittle coatings that debond within the coating. Some results obtained for three ductile- and brittle-bonded systems have provided some useful information on the role of plasticity of the coating material. For example, plastic deformation of metal coatings undoubtedly provides a contribution to the fracture energy for the metal–ceramic system. However, adequate mechanics models have yet to be developed which can properly account for the plasticity of the metal coatings.

* On leave at the Department of Mechanical Engineering, Hong Kong University of Science and Technology, Clear Water Bay, Kowloon, Hong Kong.

0022–2461

In this paper, both the plastic hardening coating and the perfectly plastic coating are considered. A theoretical model including the effect of plasticity in the coating for the single-fibre pull-out test is developed and evaluations of the interface debond and maximum pull-out stresses are given for coatings with different elastic moduli, yield stresses and thicknesses. SiC fibre–glass matrix and carbon fibre–epoxy matrix composites are used to demonstrate the effects of these plastic coatings.

2. Debonding

2.1. Fundamental equations

We consider, for simplicity, the single-fibre pull-out test in which a debonded region has extended along the fibre–coating interface (see Fig. 1). It is assumed that interfacial crack propagation induces plastic deformation in the coating of the debonded region but any plasticity at the debond crack tip is ignored. Frictional shear and radial clamping stresses are considered to exist at this debonded interface. Also there is a perfect interface bond between the coating and the matrix.

As shown in Fig. 1, the shear-lag model consists of a rod (fibre) with radius a, a cylindrical shell (coating) with thickness t and a cylindrical shell (matrix) with outer radius b, which can be determined from the fibre radius and fibre volume fraction. The fibre is located at the centre of the coaxial cylindrical shells. The z-direction is parallel to the fibre axis and the load, P, is applied at the fibre end ($z = 0$). L is the fibre embedded length and at its remote end ($z = L$), it is fixed. The coating thickness, t, is uniform along the fibre; l is the debond length, which conveniently divides the coating into two regions, elastic region (bonded region) and plastic region (debonded region).

In the debonded region, the equilibrium equations are given by

$$\frac{d\sigma_f}{dz} = -\frac{2}{a}\tau_f \tag{1}$$

$$\frac{d\sigma_l}{dz} = \frac{2}{(a+t)^2 - a^2}[a\tau_f - (a+t)\tau_e] \tag{2}$$

$$\frac{d\sigma_m}{dz} = \frac{2}{a}\tau_e \tag{3}$$

$$\sigma_a = \sigma_f C_f + \sigma_l C_l + \sigma_m C_m \tag{4}$$

where σ_f, σ_l and σ_m represent the average values of the axial stresses in the fibre, coating and matrix, respectively. $\sigma_a (= PC_f/\pi a^2)$ is the applied composite stress, P is the load exerted at the fibre end, C_f, C_l and C_m are the volume fractions of the fibre, coating and matrix, respectively. τ_e is the shear stress at the coating–matrix interface. The frictional shear stress between the fibre and coating, τ_f, is assumed constant along the debond length and is given by

$$\tau_f = \mu q_0 \tag{5}$$

in which μ is the coefficient of friction and q_0 is the initial residual stress caused by the mismatch of thermal expansion coefficients between the fibre and the coating.

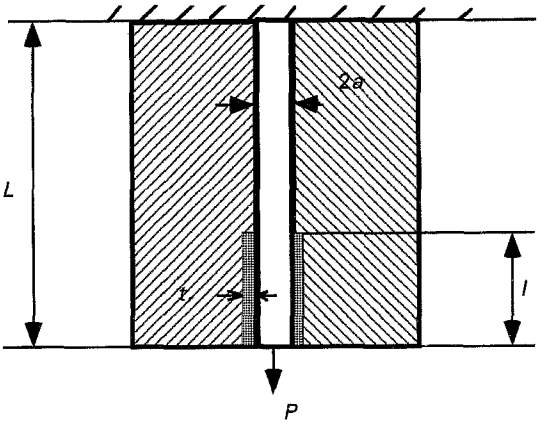

Figure 1 Schematic diagram of the fibre–coating–matrix system.

The stress–strain relationships are given by Hooke's law

$$\frac{du_f}{dz} = \frac{\sigma_f}{E_f} \tag{6}$$

$$\frac{du_l}{dz} = \frac{du_m}{dz} \tag{7}$$

$$\frac{du_m}{dz} = \frac{\sigma_m}{E_m} \tag{8}$$

where u_f, u_l and u_m are the displacements in the fibre, coating and matrix, respectively. The boundary conditions are

$$\sigma_f(0) = P/\pi a^2 \tag{9}$$

$$\sigma_l(0) = 0 \tag{10}$$

$$\sigma_m(0) = 0 \tag{11}$$

2.2. Plastic stresses and deformations in coating

To simplify the problem, three assumptions are made concerning the coating: (1) when debonding occurs, the plasticity of the coating is considered only in the debonded region; (2) Poisson's effect is neglected; and (3) the shear stresses in the coating and the matrix are neglected. Assumption 1 is made because we do not know the precise stress distributions nor the plastic zone length at the debonded crack tip. Assumptions 2 and 3 imply that the coating is subjected to one-dimensional tension. Here, two plastic constitutive models, Ramberg–Osgood and perfectly plastic models, are used to describe a plastic hardening coating and a perfectly plastic coating, respectively.

2.2.1. Ramberg–Osgood model

$$\varepsilon_l = \frac{\sigma_l}{E_l}\left[1 + \left(\frac{\sigma_l}{\sigma_s}\right)^m\right] \qquad m \geqslant 1 \tag{12}$$

where ε_l, σ_l, E_l and σ_s are, respectively, the strain and stress, the elastic modulus and the yield stress of the

coating. When σ_l is very small Equation 12 describes the elastic case; and when σ_l is large, it approximates the power-hardening rule.

2.2.2. Perfectly plastic model

$$\sigma_l = \sigma_s \tag{13}$$

By this model, no plastic hardening can occur. At the fibre end ($z = 0$), $\sigma_l(0^-) = 0$ and $\sigma_l(0^+) = \sigma_s$. Physically, σ_l increases gradually from 0 to σ_s.

2.3. Formulations of stresses and deformations in the debonded region

Integrating Equation 1 and using the boundary condition 9, as well as Equation 4, we obtain the stresses in the fibre and matrix as

$$\sigma_f = -\frac{2}{a}\tau_f z + \frac{P}{\pi a^2} \tag{14}$$

$$\sigma_m = \frac{1}{C_m}\left(\frac{P}{\pi a^2}C_f - \sigma_f C_f - \sigma_l C_l\right) \tag{15}$$

The stress in the coating by the Ramberg–Osgood model can be evaluated from Equations 7, 8 and 12. For simplicity, we consider the case $m = 1$ (although cases $m > 1$ can be derived similarly). Thus, we have

$$\sigma_l = \frac{1}{2}\left[-B + (B^2 - 4C)^{1/2}\right] \tag{16a}$$

where

$$B = \sigma_s\left(1 + \frac{E_l C_l}{E_m C_m}\right) \tag{16b}$$

and

$$C = -\frac{E_l \sigma_s}{E_m C_m}\frac{2\tau_f C_f z}{a} \tag{16c}$$

σ_l increases with increasing E_l/E_m and σ_s.

The stress in the coating by the perfectly plastic model is given by Equation 13. The displacements of the fibre and matrix in the debonded region are

$$u_f(z) = -\int_z^l \varepsilon_f \, dz = -\frac{1}{E_f}\left[-\frac{\tau_f}{a}(l^2 - z^2) + \frac{P}{\pi a^2}(l - z)\right] \tag{17}$$

$$u_m(z) = u_l(z) = -\int_z^l \varepsilon_m \, dz \tag{18}$$

(a) For the Ramberg–Osgood model

$$u_m(z) = -\frac{1}{E_m C_m}\left[\frac{PC_f}{\pi a^2}(l - z) - \frac{C_l}{2}\left(-B(l - z) + \frac{1}{6C_o} \times ([(4C_o l + B^2)^3]^{1/2} - [(4C_o z + B^2)^3]^{1/2})\right)\right] \tag{19a}$$

where

$$C_0 = \frac{E_l \sigma_s}{E_m C_m}\frac{2\tau_f C_f}{a} \tag{19b}$$

(b) For the perfectly plastic model

$$u_m(z) = -\frac{1}{E_m C_m}\left\{\left(\frac{PC_f}{\pi a^2} - C_l\sigma_l\right)(l - z) - C_f\left[-\frac{\tau_f}{a}(l^2 - z^2) + \frac{P}{\pi a^2}(l - z)\right]\right\} \tag{20}$$

Both $u_f(z)$ and $u_m(z)$ are linearly related to the external load, P, for a given debond length. The displacements in the fibre and matrix in the bonded region are equal, as there is no relative displacement, i.e.

$$u_f(z) = u_m(z) = u_l(z) = -\frac{P}{\pi a^2}\frac{C_f}{E_c}(L - z) \tag{21a}$$

where

$$E_c = C_f E_f + C_l E_l + C_m E_m \tag{21b}$$

and L is the total embedded length of the fibre. Therefore, from Equations 17 and 21, the displacement at the fibre end is

$$u_f(0) = -\frac{PC_f}{\pi a^2 E_c}(L - l) - \frac{1}{E_f}\left(-\frac{\tau_f}{a}l^2 + \frac{Pl}{\pi a^2}\right) = -\left[\frac{C_f}{E_c}(L - l) + \frac{l}{E_f}\right]\frac{P}{\pi a^2} + \frac{\tau_f l^2}{E_f a} \tag{22}$$

The relative displacement of the fibre to the matrix in the debonded region can be calculated as follows.

(a) For the Ramberg–Osgood model

$$v(z) = |u_f(z) - u_m(z)| = \left(\frac{1}{E_f} + \frac{C_f}{E_m C_m}\right)\left[-\frac{\tau_f}{a}(l^2 - z^2) + \frac{P}{\pi a^2}(l - z)\right] - \frac{1}{E_m C_m}\left[\frac{PC_f}{\pi a^2}(l - z) - \frac{C_l}{2}\left(-B(l - z) + \frac{1}{6C_o} \times \{[(4C_o l + B^2)^3]^{1/2} - [(4C_o z + B^2)^3]^{1/2}\}\right)\right] \tag{23}$$

(b) For the perfectly plastic model

$$v(z) = |u_f(z) - u_m(z)| = \left(\frac{1}{E_f} + \frac{C_f}{E_m C_m}\right)\left[-\frac{\tau_f}{a}(l^2 - z^2) + \frac{P}{\pi a^2}(l - z)\right] - \frac{PC_f/\pi a^2 - C_l\sigma_l}{E_m C_m}(l - z) \tag{24}$$

The relative displacement at the fibre end, δ, is given by Equation 22 at $z = 0$.

(a) For the Ramberg–Osgood model

$$\delta = \left(\frac{1}{E_f} + \frac{C_f}{E_m C_m}\right)\left(-\frac{\tau_f}{a}l^2 + \frac{P}{\pi a^2}l\right) - \frac{1}{E_m C_m} \times \left[\frac{PC_f}{\pi a^2}l - \frac{C_l}{2}\left(-Bl + \frac{1}{6C_o} \times \left\{[(4C_o l + B^2)^3]^{1/2} - B^3\right\}\right)\right] \tag{25}$$

(b) For the perfectly plastic model

$$\delta = \left(\frac{1}{E_f} + \frac{1}{E_m}\frac{C_f}{C_m}\right)\left(-\frac{\tau_f}{a}l^2 + \frac{P}{\pi a^2}l\right) - \frac{PC_f/\pi a^2 - C_1\sigma_1}{E_m C_m}l \quad (26)$$

The derivatives of the displacement at fibre end $u_f(0)$ and the relative displacement of the fibre to matrix v to debond length l are, respectively,

$$\frac{\partial u_f(0)}{\partial l} = \left(\frac{C_f}{E_c} - \frac{1}{E_f}\right)\frac{P}{\pi a^2} + \frac{2\tau_f}{E_f a}l \quad (27)$$

$$\frac{\partial v}{\partial t} = \frac{1}{E_f}\frac{P}{\pi a^2} - \left(\frac{1}{E_f} + \frac{1}{E_m}\frac{C_f}{C_m}\right)\frac{2\tau_f}{a}l + \frac{C_1\sigma_1}{E_m C_m} \quad (28)$$

is given by Equations 16 and 13 for the Ramberg–Osgood model and the perfectly plastic models, respectively.

3. Debonding criterion

Following Gao *et al.* [11], the progressive debonding process may be treated as crack propagation along the interface of the fibre coating, for a cracked body subjected to traction, p, acting on the boundary of surface, S_T, and friction, τ_f, along surface, S_F. The corresponding displacements are du and dv. For crack growth, dA, based on the principle of energy balance, we obtain

$$\int_{S_p} p\,du\,ds = g\,dA + \int_{S_F} \tau_f\,dv\,ds + dU_e + dU_p \quad (29)$$

where g is the specific work of fracture, $\int_{S_F}\tau_s\,dv\,ds$ is the work of friction, dU_e and dU_p represent the elastic and plastic energy of the cracked body, respectively. The elastic energy of the system can be derived as

$$dU_e = \frac{1}{2}\int_{S_p} p\,du\,ds - \frac{1}{2}\int_{S_F}\tau_f\,dv\,ds - \frac{1}{2}\int_{U_1} P_1\,du_1 \quad (30)$$

where P_1 and u_1 are the force and displacement in the coating. The plastic energy of the coating is

$$dU_p = \int_{v_1}\int \sigma_1\,d\varepsilon_1\,dv_1 \quad (31)$$

Combining Equations 29–31, we obtain the fracture criterion

$$g = \frac{1}{2}\frac{\partial}{\partial A}\int_{S_p} p\,du\,ds - \frac{1}{2}\frac{\partial}{\partial A}\int_{S_F}\tau_f\,dv\,ds + \frac{1}{2}\frac{\partial}{\partial a}\int_{U_1} P_1\,du_1 - \frac{\partial}{\partial A}\int_{V_1}\int \sigma_1\,d\varepsilon_1\,dv_1 \quad (32)$$

If there are n concentrated forces $P_1, \ldots, P_i, \ldots, P_n$ applied on S_F of the cracked body giving corresponding displacements $\delta_1, \ldots, \delta_i, \ldots, \delta_n$ Equation 32 becomes

$$g = \frac{1}{2}\left[\sum_{i=1}^{n} P_i\frac{\partial\delta_i}{\partial A} - \int_{S_F}\tau_f\frac{\partial v}{\partial A}\,ds\right] + \frac{1}{2}\frac{\partial}{\partial A}\int_{U_1} P_1\,du_1 - \frac{\partial}{\partial A}\int_{V_1}\int \sigma_1\,d\varepsilon_1\,dv_1 \quad (33)$$

Equation 33 can be applied to the fibre debonding problem shown in Fig. 1. Thus, we have $g = \zeta$, $A = 2\pi a l$, $ds = 2\pi a\,dz$ and $P_i = P$, $\delta_i = u_f(0)$, so the debonding criterion is given by

$$\zeta = -\frac{P}{4\pi a}\left(\frac{\partial u_f(0)}{\partial l}\right) - \frac{1}{2}\int_0^l \tau_f\frac{\partial v}{\partial l}\,dz + \frac{1}{2}\int_a^{a+t}\sigma_1\varepsilon_1\frac{\tau}{a}\,dr - \int_a^{a+t}\int \sigma_1\,d\varepsilon_1\frac{\tau}{a}\,dr \quad (34)$$

The physical meaning of the first two terms is the same as given by Gao *et al.* [11], i.e. the first term on the right side of Equation 34 is identical to the well-established compliance equation, the second term is the friction contribution to ζ, the third and fourth terms give the contribution of the coating (debonded region) to ζ. Although the first and second terms are the same, they are, however, affected by the coating behaviour. The debond load, P_d, (debond stress $\sigma_d = P_d/\pi a^2$) and the initial debond load, P_0 (no friction $\mu = 0$) are given by the following equations. Inserting Equations 27, 28 and 16 into 34, we obtain

$$\zeta_c = -\frac{P_d}{4\pi a}\left[\left(\frac{C_f}{E_c} - \frac{1}{E_f}\right)\frac{P_d}{\pi a^2} + \frac{2\tau_f}{E_f a}l\right] - \frac{1}{2}\tau_f l\left[\frac{1}{E_f}\frac{P_d}{\pi a^2} - \left(\frac{1}{E_f} + \frac{1}{E_m}\frac{C_f}{C_m}\right)\frac{2\tau_f}{a}l + \frac{C_1\sigma_1}{E_m C_m}\right] - \left[\frac{\sigma_1^2}{E_1}\left(\frac{1}{2} + \frac{2\sigma_1}{3\sigma_s}\right) - \frac{1}{2}\sigma_1\varepsilon_1\right]\frac{(a+t)^2 - a^2}{2a} \quad (35)$$

for partial debonding for a hardening coating. If $\mu = 0$, we obtain the initial debonding conditions

$$\zeta_c = -\frac{P_0^2}{4\pi^2 a^3}\left(\frac{C_f}{E_c} - \frac{1}{E_f}\right) \quad (36)$$

Similarly, with Equations 27, 28, 13 and 34, we obtain

$$\zeta_c = -\frac{P_d}{4\pi a}\left[\left(\frac{C_f}{E_c} - \frac{1}{E_f}\right)\frac{P_d}{\pi a^2} + \frac{2\tau_f}{E_f a}l\right] - \frac{1}{2}\tau_f l\left[\frac{1}{E_f}\frac{P_d}{\pi a^2} - \left(\frac{1}{E_f} + \frac{1}{E_m}\frac{C_f}{C_m}\right)\frac{2\tau_f}{a}l + \frac{C_1\sigma_1}{E_m C_m}\right] + \frac{\sigma_1}{4aE_m C_m} \times \left(C_1\sigma_1 - \frac{2\tau_f C_f}{a}l\right)[(a+t)^2 - a^2] \quad (37)$$

for partial debonding for the perfectly plastic coating. Again, if $\mu = 0$, we obtain

$$\zeta_c = -\frac{P_0^2}{4\pi^2 a^3}\left(\frac{C_f}{E_c} - \frac{1}{E_f}\right) + \frac{C_1\sigma_1^2}{4aE_m C_m}[(a+t)^2 - a^2] \quad (38)$$

for the initial debonding criterion. Note that when $t \ll a$, both types of coating give the same debond criterion, i.e. Equation 38 reduces to Equation 36. Physically, this means that the plastic energy absorption contribution to ζ_c is negligible.

4. Numerical examples and discussions

To illustrate the usefulness of the theories presented in the previous two sections, we select two composite systems, a SiC fibre–glass matrix composite and a carbon fibre–epoxy resin matrix composite, which are typical of ceramic- and polymer–matrix composites. Their material and interfacial properties are given in Table I and are representative of these composites. Specifically, we intend to examine the effects of the coating modulus, E_1, relative to the fibre or matrix and the coating material yield stress, σ_s, on the partial debonding stress, $\sigma_d = P_a/\pi d^2$, using Equations 35 or 37, and the maximum frictional pull-out stress, σ_p, using Equation 14 when $\sigma_f(L) = 0$ and $z = L$.

For the SiC fibre–glass matrix system, in addition to the uncoated fibre case, we consider the following coated fibre cases: (a) $E_1 = E_m$, $\sigma_s = 100$ MPa; (b) $E_1 = E_f$, $\sigma_s = 100$ MPa; (c) $E_1/E_m = 0.1$, $\sigma_s = 100$ MPa; and (d) $E_1 = E_m$, $\sigma_s = 10$ MPa. The coating thickness, t, to fibre radius, a, ratio is 0.1. These cases cover the bounds when the coating modulus, E_1, is equal to that of the fibre and less than that of the matrix. Both a large and a small yield stress are also considered.

For the carbon fibre–epoxy matrix composite, the uncoated fibre and four coated fibre cases are also considered: (a) $E_1 = E_m$, $\sigma_s = 10$ MPa; (b) $E_1/E_m = 10$, $\sigma_s = 100$ MPa; (c) $E_1/E_m = 0.1$, $\sigma_s = 10$ MPa; and (d) $E_1/E_m = 1.0$, $\sigma_s = 50$ MPa. The t/a ratio is 0.3 in these examples. Here we only include the situations when the coating modulus, E_1, is less than E_f, but can be bigger than, equal to or less than E_m.

Figs 2 and 3 show the partial debond stress as a function of debond length for the SiC fibre–glass matrix composite with a power hardening and perfectly plastic coating, respectively. Clearly, for all cases, the debond stress increases almost linearly with debond length. This seems to be caused by the ever-increasing frictional work and plastic energy dissipation in the coating as the debond length increases, because the Poisson's effect is neglected. For the same coating conditions, there is little difference in the debond stress for the linear hardening and non-hardening coating materials. It is also clear from these two figures that the debond stresses for the uncoated fibre and coated fibre cases (a), (c) and (d) are approximately equal for the same debond length. However, for the coated fibre case (b), the debond stresses are smaller. These theoretical results mean that for $E_1 \leqslant E_m$ and σ_s is identical, σ_d remains constant for a given l. Decreasing σ_s by 10 times does not have much effect on σ_d. But if $E_1 = E_f$, i.e. a coating much harder than the matrix and equal to the ceramic fibre, σ_d is reduced. So, the elastic modulus, E_1, of the coating is an important parameter in determining the debond stress, σ_d.

TABLE I Material parameters and interfacial properties of two composite systems

Material parameter/ interfacial properties	SiC fibre–glass matrix	C fibre–epoxy matrix
Fibre modulus, E_f (GPa)	400	230
Matrix modulus, E_m (GPa)	70	3
Fibre volume fraction, C_f	0.15	0.08
Fibre radius, a (μm)	100	3
Interfacial toughness, ζ_c ($J\,m^{-2}$)	50	100
Friction coefficient, μ	0.10	0.10
Residual clamping stress, q_0 (MPa)	−10	−7.0

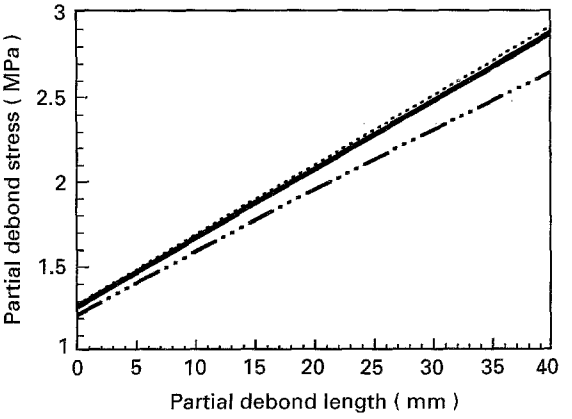

Figure 2 Partial debond stress plotted against debond length for SiC fibre–glass matrix composite in which the plastic coating is linear hardening. Coated fibre cases: (a) $E_1/E_m = 1$, $\sigma_s = 100$ MPa; (b) $E_1 = E_f$, $\sigma_s = 100$ MPa; (c) $E_1/E_m = 0.1$, $\sigma_s = 100$ MPa; and (d) $E_1 = E_m$, $\sigma_s = 10$ MPa. (————) Uncoated, (——) coated (a), (— — —) coated (b), (– – –) coated (c) (—·—) coated (d).

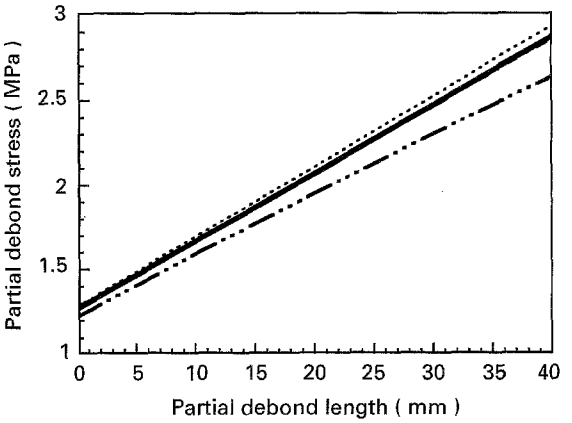

Figure 3 Partial debond stress plotted against debond length for an SiC fibre–glass matrix composite in which the plastic coating is non-hardening. For key, see Fig. 2. Coated fibre cases are identical to Fig. 2.

Figs 4 and 5 show similar σ_d results for the carbon fibre/epoxy resin composites for the linear hardening and non-hardening coating, respectively. Again, similar conclusions can be drawn as the SiC fibre–glass matrix composite system. For $E_1 \leqslant E_m$, σ_d is approximately equal though the coated fibre case (c), where $E_1 = 0.1\ E_m$ shows a slightly higher value at a given debond length. The coating yield stress is not as

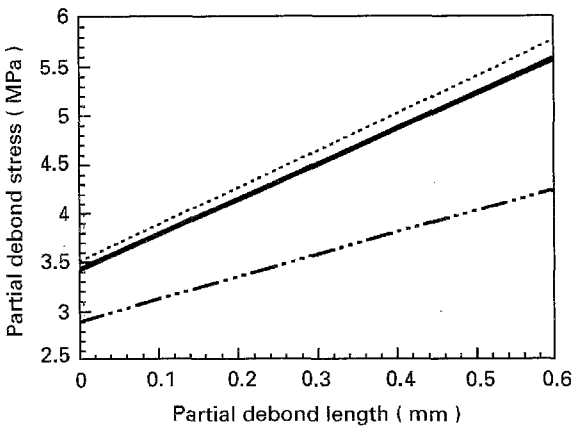

Figure 4 Partial debond stress plotted against debond length for a carbon fibre–epoxy matrix composite for a linear hardening plastic coating. Coated fibre cases: (a) $E_1 = E_m$, $\sigma_s = 10$ MPa; (b) $E_1/E_f = 10$, $\sigma_s = 100$ MPa; (c) $E_1/E_m = 0.1$, $\sigma_s = 10$ MPa; and (d) $E_1 = E_m$, $\sigma_s = 50$ MPa. For key, see Fig. 2.

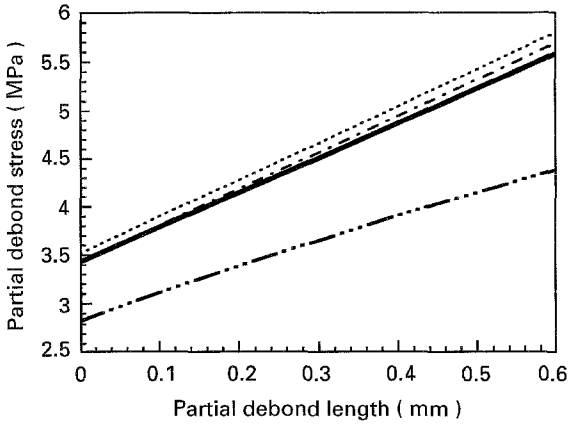

Figure 5 Partial debond stress plotted against debond length for a carbon fibre–epoxy matrix composite for a non-hardening plastic coating. Coated fibre cases are identical to Fig. 4. For key, see Fig. 2.

important. When $E_1 > E_m$, σ_d has been reduced for any l. The reduction is, however, more remarkable than the SiC–glass composite. The linear increase in σ_d with l can be explained in the same way.

Summarizing Figs 2–5, it appears that for a given interface toughness, and given thickness and yield stress of the coating, the debond stress increases almost linearly with debond length. Increasing the modulus of the coating above that of the matrix has the net effect of decreasing the debond stress. On the other hand, decreasing the coating modulus slightly increases the debond stress. Physically, this means a more compliant plastic coating with a higher yield stress is required to control interfacial debonding. It would therefore seem that a thick coating is more effective than a thin coating to increase the debond stress. However, the effect of the coating thickness has not been studied yet in this work.

The maximum frictional pull-out stress, σ_p, as a function of embedded fibre length, L, is given in Figs 6 and 7 for the two types of composites. The linear hardening or non-hardening nature of the coating material is unimportant. And according to Equation 14 with $\sigma_f(L) = 0$ and $z = L$, it is expected that σ_p

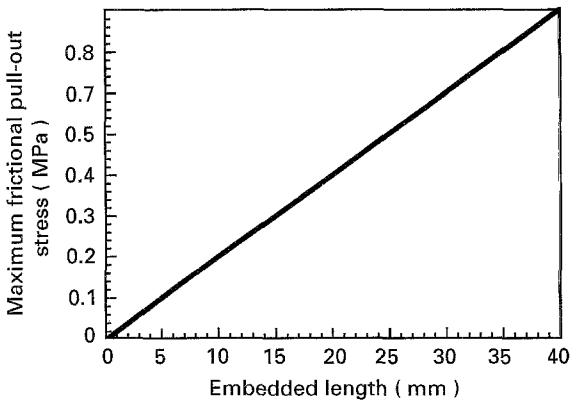

Figure 6 Maximum frictional pull-out stress plotted against fibre embedded length for the SiC fibre–glass matrix composites. Results are identical for linear hardening and non-hardening coatings and all cases studied in Figs 2 and 3.

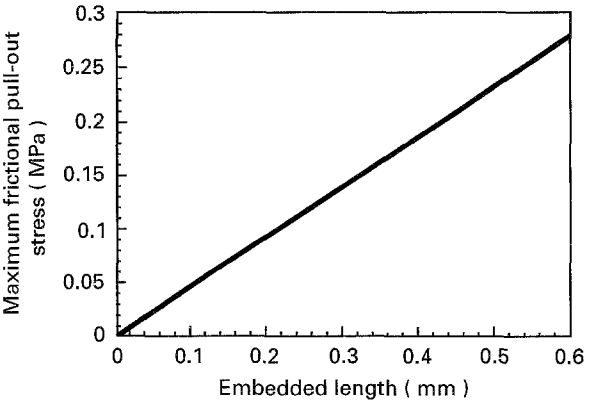

Figure 7 Maximum frictional pull-out stress plotted against fibre embedded length for the carbon fibre–epoxy matrix composites. Results are the same for linear hardening and non-hardening coatings and all cases studied in Figs 4 and 5.

depends linearly on L and $\tau_f(=\mu q_0)$. No properties of the fibre coating come into the equation. Again this result is expected, and is because we have not considered the Poisson's effect on stretching the fibre. Hence, the coating will not affect the maximum frictional pull-out stress.

5. Conclusion

A theoretical model is presented for the interfacial debonding and frictional pull-out of a single elastic fibre which is coated with a plastic coating from an elastic matrix. A new debond criterion has also been established for a linear hardening and a non-hardening plastic coating. Parametric studies on two composite systems, a SiC fibre–glass matrix composite and a carbon fibre–epoxy matrix composite, show that increasing the yield stress and decreasing the elastic modulus of the coating improve the debond stress at any debond length. The maximum frictional pull-out stress is dependent linearly on fibre embedded length but independent of the coating properties. The analytic solutions provided in this paper are exact and correct for the assumptions made in Section 2.2. Also, because Poisson's effects are neglected in the analysis, the solutions apply equally to fibre push-out.

Acknowledgements

Y.-W. Mai thanks the Australian Research Council (ARC) for the continuing support of this project. G.-Y. Lu was financially supported by the ARC when this work was initiated at Sydney University.

References

1. A. G. EVANS, F. W. ZOK and J. DAVIS, *Compos. Sci. Technol.* **42** (1991) 3.
2. A. G. EVANS, M. RUHLE, B. J. DALGLESH and P. G. CHARALAMBIDES, *Mater. Sci. Eng.* **A126** (1990) 53.
3. J. D. H. HUGHES, *Compos. Sci Technol.* **41** (1991) 13.
4. J. -K. KIM and Y. -W. MAI, *J. Mater. Sci.* **26** (1991) 4702.
5. *Idem, Compos. Sci. Technol.* **41** (1991) 333.
6. T. W. CLYNE and M. C. WATSON, *ibid.* **42** (1991) 25.
7. A. DI'ANSELMO, M. L. ACCORSI and A. T. DIBENEDETTO, *ibid.* **44** (1992) 215.
8. S. M. CONNELLY, M. L. ACCORSI, A. T. DIBENEDETTO and A. DI'ANSELMO, in Proceedings of the Fifth European Conference on Composite Materials, Bordeaux, France, edited by A. R. Bunsell et al. (EACM, 1992).
9. N. R. SOTTOS, R. L. McCULLOUGH and W. R. SCOTT, *Compos. Sci. Technol.* **44** (1992) 319.
10. S. K. MITAL and C. C. CHAMIS, *J. Compos. Technol. Res.* **13** (1991) 14.
11. Y. C. GAO, Y. -W. MAI and B. COTTERELL, *J. Appl. Math. Phys. (ZAMP)* **39** (1988) 550.

Received 9 May
and accepted 7 June 1995